Flood hazard assessment in a polje: the case of Mucille (Classical Karst Region, NE Italy)

Zini Luca[1] · Calligaris Chiara[1] · Forte Emanuele[1] · Turpaud Philippe[1]

Abstract

The Mucille karst depression is one of the few examples of polje on the Italian side of the Classical Karst Region, a shared area between Italy and Slovenia. The polje is subject to frequent flooding, becoming more problematic since 2000, as swallow holes more frequently have affected housing and recreational areas, leading the population to believe that their ability in draining the area had stopped functioning. Climate changes play an important role as there has been an intensification in extreme events (30-day cumulative precipitation of more than 350 mm) within the considered time-period 1919–2020. The necessity to provide answers to the inhabitants required in-depth studies such as hydrogeological investigations, discharge measurements and Electrical Resistivity Tomography (ERT) acquisitions. Over the 3 years of monitoring (2017–2020), two flood events reached the Selz settlement. In total, four events have been analysed to build a hydrogeological model of the area in order to properly estimate its recharge and regression curve, and to define the functionalities of the swallow holes. The defined model allowed a better knowledge and a greater awareness in proposing the proper mitigation measures able to increase the drainage capacity of the area avoiding always more frequent future floodings.

Introduction

The rapid infiltration of rainwater is one of the defining characteristics of karst areas to the extent that surface watercourses are rarely present in these barren territories (Ford and Williams 2007). Fractures and conduits enlarged by karst processes allow for rapid water transfer from the surface into the aquifer, and if the spring areas are not developed enough to drain all the infiltrating water, a rapid rise in piezometric levels is observed. Under such conditions these levels can rise tens of metres in a few hours (Zini et al. 2014; Filippini et al. 2018; Gabrovšek et al. 2018) leading to the flooding of the most depressed areas by forming the so-called ephemeral or intermittent lakes (Long et al. 2014; Parise et al. 2015; Mayaud et al. 2019; Morrissey et al. 2020; Watlet et al. 2020; Ravbar et al. 2021).

As is well-known, ongoing climate change is leading to the significant alteration in the precipitation regime and to a general increase in the frequency of short, but very intense precipitation (EEA 2016). Over the last decades, this intensification in extreme events led to an increasing number of invasive and destructive floods (Hirabayashi et al. 2013; Parise 2015; Kvočka et al. 2016; Tabari 2020). Karst areas are no exception, as they represent a fragile environment that is sensitive to hydrometeorological and geological hazards (Margiotta and Parise 2019). The rainfall regime heavily impacts on the permanence of water in these ephemeral lakes and on the flooding patterns which are highly variable and linked to precipitation (Lopez-Chicano et al. 2002; Gracia et al. 2003; Lopez et al. 2009).

The Friuli Venezia Giulia Region (NE Italy) is one of the rainiest regions in Italy with an average rainfall between 1.000 mm/year on the coast and 2500/3000 mm/year in the pre-Alpine area, and is not immune to the effects of climate change. The forecast made by the ICPT (ARPAFVG 2018), comparing the time span 1970–2005 with that of 2006–2100 confirms the observed trends and predicts general increases in temperature with values in the wintertime ranging from + 1.3 to + 5.3 °C, up to almost + 6 °C in the summer. With regard to precipitation, an increase of 20–30% is expected in the winter and a decrease, albeit moderate,

✉ Calligaris Chiara
  calligar@units.it

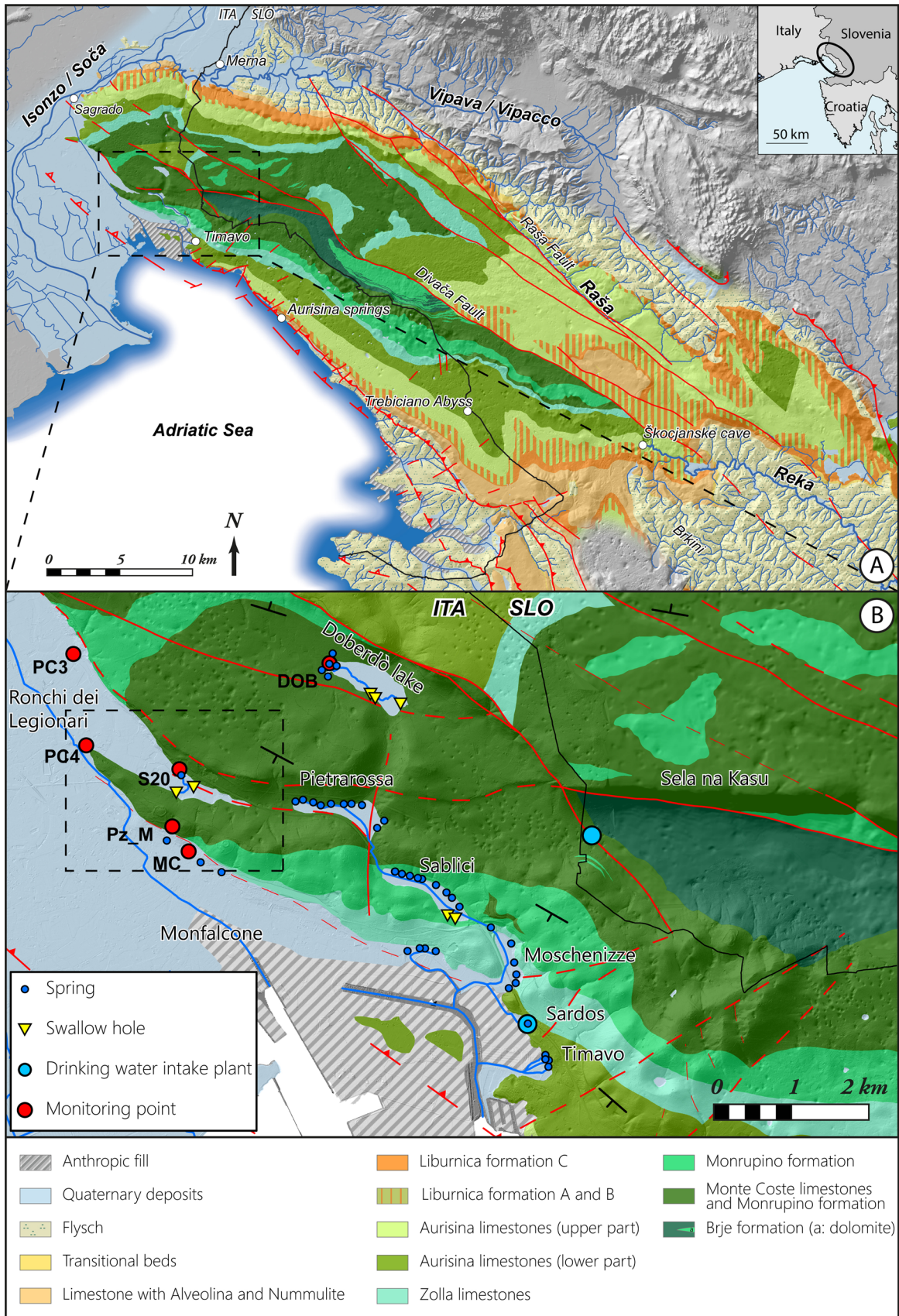1   Dipartimento di Matematica e Geoscienze, Università degli Studi di Trieste, Trieste, Italy

◄**Fig. 1 A** Simplified geological map of the Classical Karst Region (Jurkovšek et al. 2016). **B** The westernmost part of the Classical Karst Region. In B, dashed black line outlines the Mucille study area

during summer. In accordance with the increase in precipitation during winter, a significant increase in extreme events is also expected, i.e. those with precipitation above the 95th percentile of the daily precipitation distribution (ARPAFVG 2018).

One of the best-known karst areas in the world is the Classical Karst Region (Jurkovšek et al. 2016), an area shared between two countries, Italy and Slovenia and called Carso and Kras in their respective countries (Zini et al. 2022). The Mucille polje is located on the Italian side of the area and is representative of the ongoing changes in the hydrogeological regime and the flood dynamics in such a particular environment. In the context of a mature and well-developed karst, these areas, where waters freely flow, represent an extraordinary resource that has always attracted the attention of man, who has in turn exploited this environment for economic and settlement purposes.

In the present study, we have focused on the Mucille area, located in the NW sector of the Classical Karst Region. The word Mucille comes from the Slovene moč, močilo indicating a swampy, marshy place. This area has always been affected by flooding, but since the end of the 1990s there has been an increase in the frequency of the events which also reached the inhabited area. After a number of land reclamation works which modified and reduced the swallow hole pertinence areas, the local population was largely of the opinion that they were no longer functioning properly.

The present study sought to understand the recharge patterns of the polje through the elaboration of a hydrogeological model during flood events, to verify the drainage capacity of the area, and to identify possible mitigation measures to reduce the flood risk in the area.

Study area

Geomorphological, geological and structural setting

The Classical Karst Region, extending from the Soča/Isonzo River plain to the northwest, to the Adriatic Sea to the southwest and surrounded by the non-karst Vipava Valley and Brkini Mountain to the East in Slovenia (Fig. 1), covers approximately 750 km². The plateau altitudes range from one hundred metres in correspondence with Doberdò del Lago village in the NW, up to 400–450 m a.s.l. at Divača and Škocjan to the SE. With its peculiar geological characteristics, the Classical Karst Region represents the essence of karst environments (Zini et al. 2022). The waters during

the last fifteen million years eroded the flysch cover, dissolving millions of cubic metres of limestone, thus creating its unique morphologies. Furthermore, the geological and structural settings heavily condition the surface karst morphotypes, as well as those underground. In this context, the most characteristic morphological element is certainly represented by dolines, which give the topographical surface an irregular and tormented appearance. Dolines are of all sizes, with a prevalence of those with a diameter less than 50 m. There are bands in which large and deep dolines prevail, also aligned along well-defined directions, most often N–S and at times NW–SE. The rest of the territory presents a patchy distribution with a density between 40 and 75 dolines per km² (Zini et al. 2015; Cucchi et al. 2015). The latter is precisely the case of the Doberdò del Lago area where the phenomena are quite similar in size and have a density close to the maximum values. In the whole karst plateau, more than 32,817 phenomena have been recognised with a relative doline area of 11.6% (Mihevc and Mihevc 2021). There is also a significant number of known hypogean features. Speleologists from both countries have been very active over the years, and have inventoried more than 4000 caves. In Italy there are 128 caves with a development higher than 100 m, while in Slovenia there are 116. Among the whole dataset, only a dozen has a development of more than 1000 m. There are numerous cave entrances in the Monfalcone-Gorizia area, almost all of which are, however, of modest dimensions.

The structural imprinting is evident in the entire study area. It is particularly clear in the depressions hosting the Mucille Plain, Doberdò and Pietrarossa lakes, base-level poljes NW–SE oriented connected to the Colle Nero fault, a western extension of the Brestovica and Jamlje faults.

From a geological point of view, the area is characterised by a lithostratigraphic sequence going from the Lower Cretaceous to the Eocene. As defined by Vlahović et al. (2005) and by Velić (2007), the Classical Karst Region is made up of sedimentary rocks of the former Adriatic-Dinaric Carbonate Platform. The sequence is the evidence of a complex paleo-environmental evolution which involved the platform by causing it to pass through several marine-lagoon phases alternating with emerging ones, up to the final drowning. The succession of rocks, nearly 1500 m thick, has been subdivided into several geological units which group genetically related rocks together. Most of these exposed rocks are limestone, although there is also dolomite. The youngest rocks identified in the area are the sandstones and the marlstones of the Flysch of Trieste (Zini et al. 2022).

The Mucille depression is laid on a Cretaceous bedded limestone of the Monte Coste limestones and Monrupino formations (Cucchi and Piano 2013; Jurkovšek et al. 2016; Zini et al. 2022). It is an elongated sub-planar depression which lie in a NW–SE direction, approximately 200–500 m wide with altitudes degrading from W to E from 10 m a.s.l.

to 6 m a.s.l. A hump reaching 15 m a.s.l. separates it to the E from Pietrarossa Lake and a ridge rising to an altitude of approximately 100 m a.s.l. separates it from the plain to the S. A hump transversal to the depression, with an average elevation around 8 m a.s.l. divides the most depressed area into two sectors: the Selz settlement (Fig. 2 letter A) and the riding school (Fig. 2 letter B). Three old clay quarries located in the westernmost sector of the depression form small artificial lakes (Fig. 5, letter Q).

Hydrogeological setting

Two hydrogeological units characterise the Classical Karst Region aquifer: carbonate rock which are extremely karstified and permeable due to fissures and karst processes, and flysch deposits showing a very low permeability. The difference in permeability between these two units plays an important role in recharge, flow and outflow of groundwaters from the system. The marly arenaceous units bounding the carbonates act as barriers guiding not only the karst development, but also the flow of groundwater.

The entire spring system is mainly supplied by three different contributions: effective infiltrations (called *karst waters* according to Gemiti 1994, Doctor 2008 and Calligaris et al. 2019a), the sinking recharge of the Reka and Raša Rivers, and leakage from the Vipacco and Soča/Isonzo aquifers.

The Classical Karst Region is located between the Mediterranean and continental climate with an average rainfall between 1000 mm/year (along the coast) to about 1800 mm/year (inland). For this reason, rainfalls, and specifically effective infiltrations, represent the main contribution to the groundwater recharge with an estimated value of 21 m^3/s (Civita et al. 1995).

The contribution of the Reka River (Timavo Superiore) is estimated to be on average 8 m^3/s (Gabrovšek and Peric 2006) with almost negligible flow rates in low water conditions (0.18 m^3/s) but particularly intense discharges during floods (more than 300 m^3/s). In the north-western sector between the small towns of Merna and Sagrado, the aquifer of the Soča/Isonzo plain joins the *karst waters* (Timeus 1928; Mosetti and D'Ambrosi 1963; Gemiti and Licciardello 1977; Cancian 1987; Doctor et al. 2000; Samez et al. 2005; Treu et al. 2017; Calligaris et al. 2019a). In this area, the Soča/Isonzo contribution to the groundwaters is not constant throughout the year and is dependent upon the hydrogeological regime. During low flow periods, the Soča/Isonzo contribution prevails and its influence can be observed throughout the entire spring system, from Mucille to the Timavo. On

Fig. 2 Sw-02 swallow hole is the southernmost one in the study area. The discharge pipe is visible in the photo, taken on 13th November 2018 and 27th March 2018. The photographs illustrate the situation in the Sw-02 at different water levels. The water level measurements allow for the calculation of the surface water volume and consequently the daily mean water balance

average, a supply from the Soča/Isonzo waters has been estimated to be about 10 m^3/s (Zini et al. 2014; Vizintin et al. 2018; Calligaris et al. 2019b). The genesis and development of the conduit network that drains the waters from the infiltration areas towards the springs has been and is significantly influenced by the different nature of these contributions. Some large conduits from the Škocjan sinkhole drain the waters into different branches with free-surface waters, underwater drowned segments and conduits below sea level which efficiently connect the cave with the Aurisina, Timavo and Sardos spring systems. In the western sector of the Classical Karst Region, on the other hand, the waters from the Soča/Isonzo aquifer are drained towards the springs by numerous interdependent conduits mainly developed in the saturated zone below sea level. Conduits with different hydraulic conductivity are in turn connected with the system of caves and fractures which drive precipitation in the whole karst system. The influence of the Reka River is felt throughout the entire eastern sector of the Italian side of the Classical Karst Region, and is clearly observed in all springs from Aurisina to Timavo, as well as during the most intense floods at the Sardos spring, but not in the western sector where the other contributions prevail. The waters flowing in the westernmost areas are fundamentally due to two contributions: leakage from the Soča/Isonzo and Vipacco Rivers, which have an average electrical conductivity (EC) (25 °C) of 270 μS/cm, and the effective infiltration (*karst waters*), with average values of 530 μS/cm. The EC monitoring in correspondence with different sites between Sagrado and San Giovanni di Duino made it possible to observe how, depending on the hydraulic regime, one contribution prevails over the other (Calligaris et al. 2018, 2019a). During periods of low water flow, moving from west to east, a gradual increase in the groundwater EC values can be observed, confirming the importance of the water supply from the Isonzo–Vipacco system with respect to the *karst waters*. During floods, a decidedly different behaviour is observed: precipitation quickly infiltrates the karst system, increasing the hydraulic gradient, which significantly inhibits or limits the supply by the Isonzo–Vipacco system. At all water points, a sudden increase in EC values is observed (piston effect), which remains high until the water level returns to previous conditions. The Sardos spring thus represents the point of contact between the western Isonzo–Vipacco system and the eastern system linked to the Reka/Timavo: during the most intense peaks, the typical Reka signal is observed with a drop in EC.

West of the Timavo and Sardos springs, a series of polje, NW–SE oriented, placed at altitudes of between 5 and 2 m a.s.l., is present, containing intermittent lakes (Doberdò, Pietrarossa and Sablici). The Pietrarossa and Sablici area was significantly altered in the post-World War II period by a series of land reclamation works that led to a general lowering of the water table level. The Mucille depression is found within this hydrogeological context (Figs. 1 and 6), an area laid on a gently SSW dipping bedded limestone fed by a spring area. The Selz settlement (Fig. 6A) has suffered less human intervention than the riding school (Fig. 6B) and has retained a certain amount of naturality even if the waters of the two springs (S-02 and S-03) and the estavelle (S-01) present in area A have been channelised towards the swallow holes.

During low water conditions, when only S-02 is active, the flow is channeled partially towards the estavelle (S-01) and partially to the swallow hole (Sw-01). During floods, a second swallow hole (Sw-02) contributes to draining the area. In the previous century this swallow hole was subject to significant modifications for agricultural purposes and for the construction of a small discharge drainage pipeline built for the maintenance of the Trieste water supply pipeline (Fig. 2). These works reduced the swallow hole pertinence areas.

At the riding school sector (B), a temporary spring (S-04) activates during floods creating an ephemeral watercourse flowing into the Sw-03 swallow hole.

The minimum elevations within the Mucille depression are encountered along the channel connecting the spring area (4.8 m a.s.l.) to the swallow holes (4.5 m a.s.l.). The rest of the area is almost flat with elevations ranging from 6.0 to 10 m a.s.l. The lower groups of houses can be found at 7.5 m a.s.l. in area B and at an elevation of between 8.1 and 8.8 m a.s.l. in area A, respectively.

Methods

Field-survey activities including manual monitoring of the water level (WL), electrical conductivity (EC) and temperature initially facilitated the defining of the hydrogeological characteristics of the study site. EC and temperature were measured by means of a WTW Portable Conductivity Meter ProfiLine Cond 3110, T measuring range 0–80 °C, accuracy ± 0.1 and resolution 0.1; EC measuring range 10 μS/cm to 20 mS/cm, accuracy ± 0.5% and resolution 1). Adjacent to the potential flooded area, a piezometer (S20, Fig. 1) is present. Between 2017 and 2019, manual repeated measures were collected here and a multiparametric probe was installed. The probe is a CTD-Diver datalogger (Van Essen Instruments) with a pressure range of 10 m (accuracy ± 0.5 cm, resolution of 0.2 cm); the temperature ranges between − 20 °C to + 80 °C (accuracy ± 0.1 °C, resolution 0.01 °C) and the EC ranges between 0 to 120 mS/cm (accuracy ± 1%, resolution ± 0.1%). The compensation of the atmospheric pressure variability was ensured by a Baro-Diver from Van Essen (pressure range 150 cm,

accuracy ± 0.5 cm, resolution 0.03 cm) (Van Essen instruments 2023).

In order to quantify the discharges in the system, a total of 13 direct discharge measurements were carried out at various significant points/sections. All measurements were performed using an electromagnetic current meter OTT MF Pro equipped with a depth sensor. If the depth was higher than 30 cm, the subsection method was applied by measuring the outflow velocity at three different depths in a single measuring station. Stations were spaced 20–10 cm apart. The measurements took place in the channels which convey waters from the quarry lakes and springs to the swallow holes. In particular, regarding area A, measurements can be taken if the water level does not exceed 6.4 m a.s.l. When the level exceeds 6.4 m a.s.l., the water overflows the channels and direct measurements become impossible. Flow measurements were acquired during two moderate floods which occurred between February and June 2019. In sector B, the measurements were taken only when the spring activates.

While discharge measurements are possible in low-water conditions, during floods the assessment of springs and swallow hole discharge in sector A is impossible. In the latter case, Digital Terrain Models (DTMs) are helpful to calculate the water volume. By comparing the ground level and lake level elevations formed in the polje, it was possible to calculate the water volume accumulated in the depression over time. The water volume increments are the result of the flow difference between the springs (Q_{in}) and the swallow holes (Q_{out}). From DTM data, the volume of water contained in the depression was calculated in 10 cm increments. The relationship between the water level measured at S20 piezometer and the volume of water accumulated in the depression was calculated. This relation can be described by means of 3 s-order polynomial equations, respectively, in the intervals 4.8–5.6 m a.s.l. (Eq. 1), 5.6–6.3 m a.s.l. (Eq. 2), and 6.3–7.6 m a.s.l. (Eq. 3) (Fig. 3):

$$L_t = -2.93399 \cdot 10^{-8} V_t^2 + 2.84561 \cdot 10^{-4} V_t + 4.89118, \tag{1}$$

$$L_t = -5.75327 \cdot 10^{-10} V_t^2 + 4.83630 \cdot 10^{-5} V_t + 5.36650, \tag{2}$$

$$L_t = -2.98995 \cdot 10^{-11} V_t^2 + 1.53426 \cdot 10^{-5} V_t + 5.88389. \tag{3}$$

Based on the aforementioned equations, a hydrogeological model was developed using tabular data sheets. Water levels acquired in correspondence with the S20 piezometer represent the input data, and the output are the water volumes.

The model does not allow for a direct assessment of the inflow (Q_{in} from the springs) and outflow (Q_{out} from the swallow holes), but only their difference (Q_{diff}).
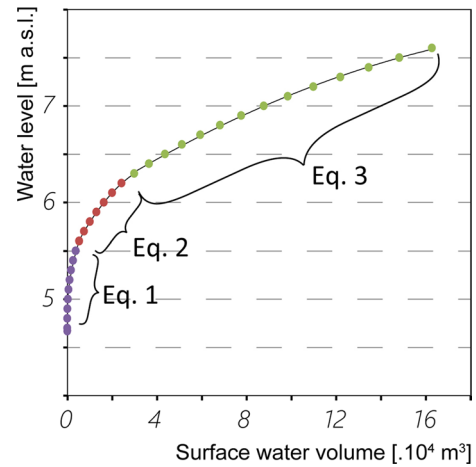

Fig. 3 Relationship between the water level measured at S20 piezometer and the volume of water accumulated in the sector A of the Mucille depression

Nevertheless, it facilitates the understanding of how the Mucille depression floods and empties (in time and volume) over times. Q_{diff} was calculated daily in an iterative manner by resetting the difference between the measured water level value in S20 and the water level calculated through the equation:

$$\text{Level} = f(\text{vol}). \tag{4}$$

Using a time-discretisation analysis, we were able to estimate, daily changes in the lake level, and thus volumes that are related to Q_{diff} by means of the following equation:

$$\Delta V = Q_{diff} \times \Delta t. \tag{5}$$

In order to evaluate the groundwater flow direction out of the system, on September 13th 2018, in low-flow conditions, 100 kg of NaCl were injected in correspondence to the Sw-02 swallow hole. EC and water level at the injection point, at the covered market in Monfalcone and in the piezometer S20 were measured by using CTD data-logger devices (Van Essen Instruments). The salt injection started at 11:00, with a concentration peak of 16,200 μS/cm at 11:37, and finished around 12:00.

In order to estimate the depth to the carbonate bedrock and to highlight the possible presence of cavities, electrical resistivity tomography (ERT) investigations were performed on April 20th (ERT1 and ERT2) and on September 13th (ERT3 and ERT4) 2018 (Fig. 4). ERT profiles were collected with a Syscal Pro (Iris) instrument with a 48 electrode cable. ERT1, ERT2 and ERT3 profiles had the electrodes spaced 1 m apart, while in ERT4 the electrodes were spaced 2 m apart. ERT3 was repeated 7 times within the dye-trace experiment. All ERT data were collected with Wenner (W) and Wenner–Schlumberger (WS) configurations. The
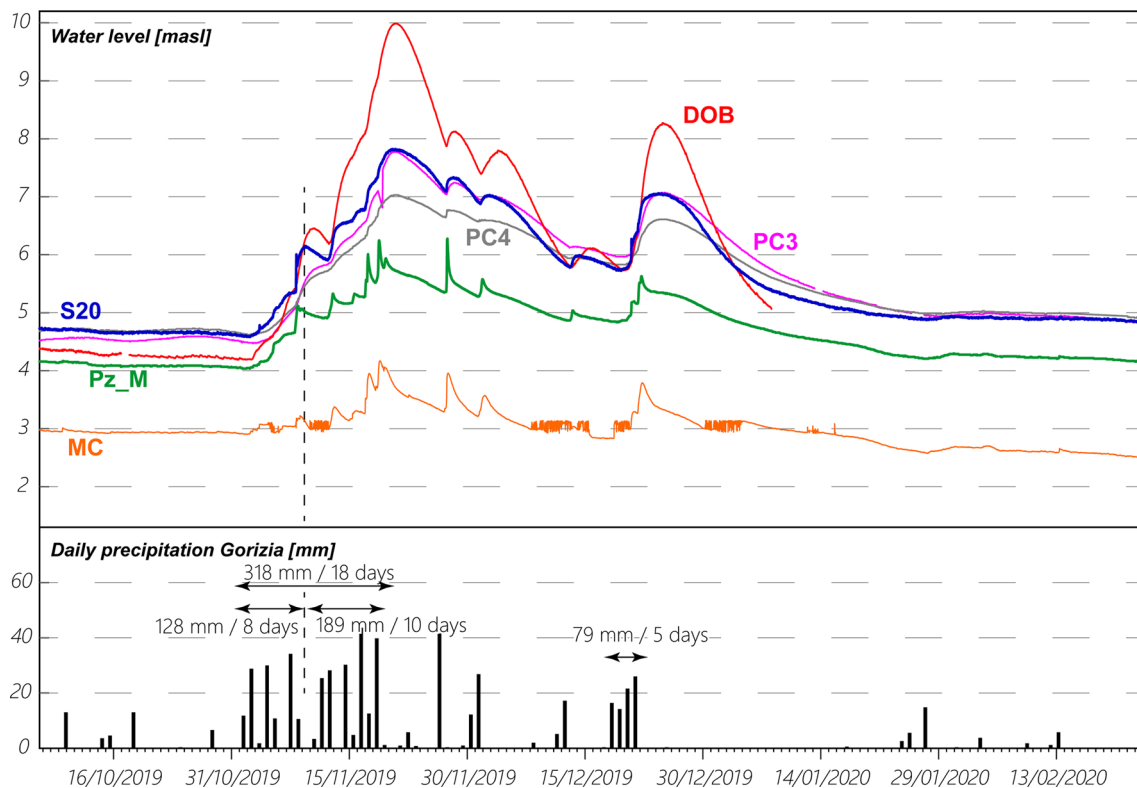
Fig. 4 Water level dynamics recorded by the multiparametric devices installed in the western sector of the Classical Karst Region at Doberdò Lake (DOB), Mucille-Monfalcone area (S20, PC3, PC4 and Pz_M piezometers) and at Monfalcone spring (MC). The lower part of the graph is related to the rainfall recorded at the Gorizia meteorological station and analysed from October 2019 to February 2020, during a flood event at the Mucille area

profiles were edited using ProsysII (version 3.14) software and inverted with both Res2Dinv (version 4.9) and ErtLab Studio modules in order to obtain an estimate of the distribution of real electrical resistivity values in the subsoil. As the area is essentially sub-flat, it was not necessary to take topography into account.

Results

Between July 2017 and April 2020, 20 water points scattered around the study area were monitored. Water level, temperature and EC data were acquired manually or by using CTD data-logger devices. Water levels show fluctuations in accordance with the recorded precipitation. Abundant rainfall is generally observed during winter, but also during spring (May 2019). Figure 4 represents an extract of the data series analysed. Summer is characterised by low rainfall and high evapotranspiration, and generally showed the lowest levels. Low levels may also occur during dry winters such as in January 2019. The continuous monitoring of the S20 piezometer allows for the description of the water table trend in the Mucille area. Within the throughout studied period (2017–2020) the water table level ranged between 4.41 and 7.82 m a.s.l. with values lower than 5 m a.s.l. recorded during most of the year (mode of 4.66 m a.s.l.). Within the 3 years of monitoring, two flood events reached the Selz settlement, in December 2017 and November 2019. Spring S-02 and swallow hole Sw-01 remain active throughout the year, while swallow hole Sw-02 activates only when the level rises above about 5.20 m a.s.l. As can be seen in Fig. 4, the monitored points show similar behaviour. During very low flow conditions (e.g. October 2019), the water level dropped to 4.4 m a.s.l. at the Mucille area (S20) and to 4.2 m a.s.l. at Doberdò (DOB). From there on, the water level very slowly decreased towards the SE reaching about 3.0 m a.s.l. near Monfalcone (MC). During floods the fast infiltration of the waters in the karst area result in an equally fast rise in the discharge at the springs and consequently the depressed areas become flooded. During the discharge peak in November 2019, the water level at Doberdò rose for about 7 m in 18 days exceeding the elevation of 10 m a.s.l. At the same time at Mucille the water level increased 3.4 m, reaching 7.82 m a.s.l., and at Monfalcone it rose about one metre reaching an elevation just over 4 m a.s.l.
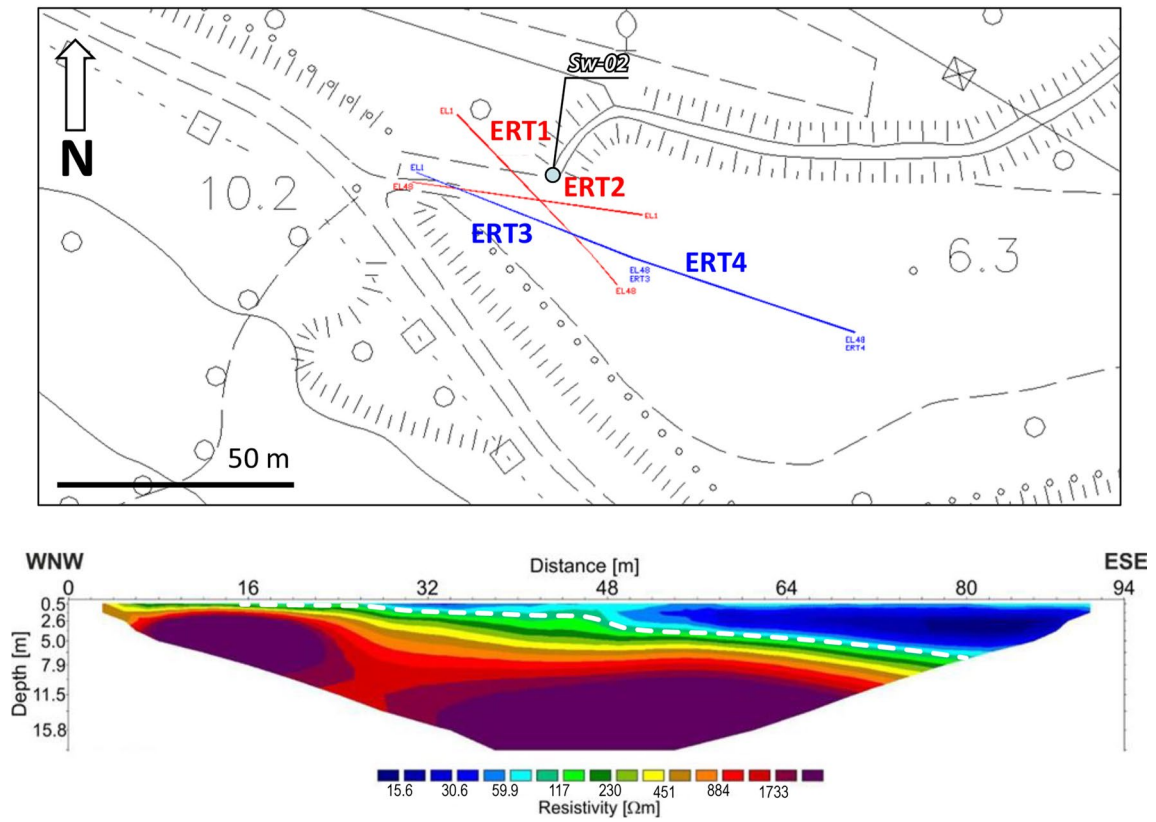
Fig. 5 Example of inverted electrical resistivity profile ERT4. The dashed white line marks the approximated depth of the limestone. Wenner–Schlumberger (WS) profile, iteration 4, RMS mean error 3.3%
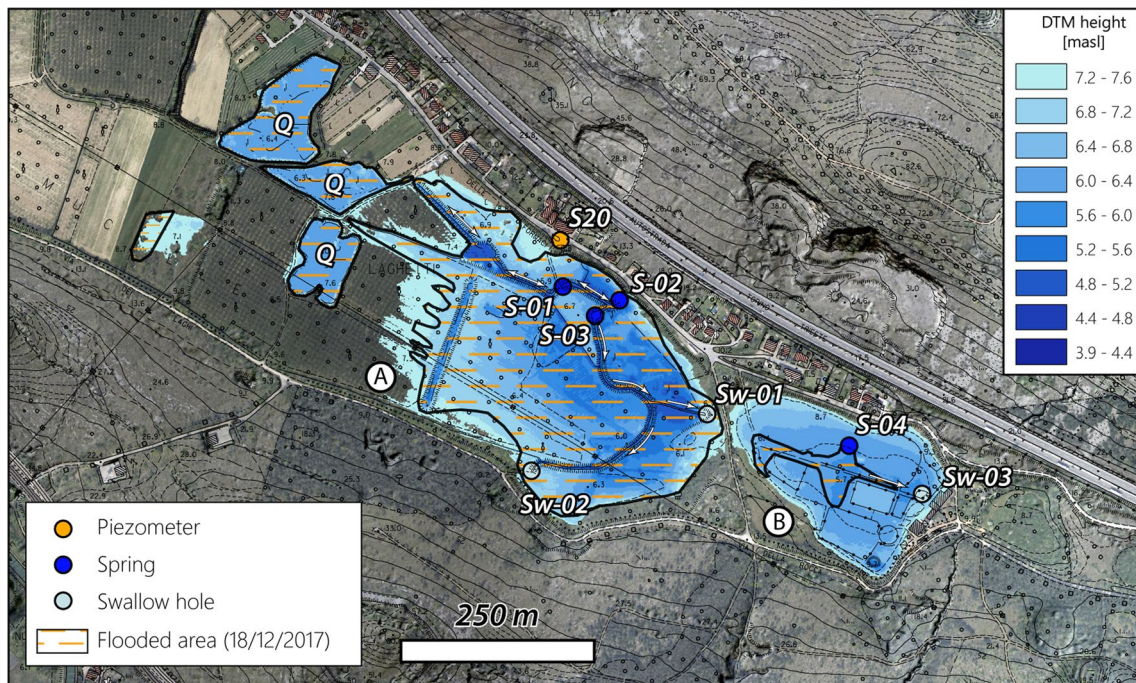

Fig. 6 Composite aerial photograph of the Mucille area. The spring area, swallow holes and monitoring piezometer are highlighted. The surface which flooded on 18th December 2017 is mapped. **A** is related to the Selz settlement depressed area, **B** to the riding school area

The rising and recession limbs related to Pz_M and MC differ from those of the whole other monitored points. This is due to the hydrogeological context in which each measuring point is located. Pz_M and MC are linked to high permeability karst conduits which allow for a fast increase and decrease in groundwater levels resulting in a faster response to the precipitation events and in sharper rising and recession limbs. DOB and S20 record the water level of karst lakes in which the swallow hole drainage capacity is lower than the spring recharge. An ephemeral lake formed which empties only when the hydraulic gradients decrease downstream. Thus the rising and recession limbs appear to be smoothed and wider. PC3 and PC4 demonstrate a similar behaviour to the karst lakes as piezometers were placed in an alluvial plain aquifer with a lower permeability with respect to the karst conduits.

In order to verify the efficiency of swallow hole Sw-02 and to understand the extent of the impact related to the land reclamation works, a campaign of ERT acquisitions was carried out to determine the thicknesses of the clayey silt deposits and the bedrock characteristics. The investigations were acquired transversally to the direction of the drainage channel (Fig. 5). ERT data provided interesting results about the depth and nature of the calcareous bedrock. In detail, the ERT4 profile (Fig. 5) demonstrates that below a low-resistivity horizon referred to the topsoil, a marked increase in electrical resistivity is observed with values close to 2,000 Ohm x m, attributable to limestones under water-saturated conditions. Close to the swallow hole the bedrock is only a few decimetres from the topographic surface, but moving eastwards it deepens to approximately 7 m. Conversely to the geomorphology of the area, this datum, which in this sector of the polje is sub-horizontal at an elevation of approximately 6 m a.s.l., is in agreement with the observations made in the proximity of the swallow hole where some fractures draining water are observed on the eastern bank.

A tracer test was also performed to determine into which spring sector the waters swallowed by swallow hole Sw-02 were drained. In September 2018, 100 kg of sodium chloride, previously dissolved in water, was injected into swallow hole Sw-02. The injection lasted one hour. At the same time, Monfalcone (MC), Pietrarossa, Sablici, Moschenizze, Sardos and Timavo springs were monitored in continuous by CTD data-logger devices. After 22 h from injection, the tracer was detected at the springs of Monfalcone. The concentration peak was reached 12 h after the first detection. The linear distance between the two points is 700 m. Based on this distance, a maximum and average transit velocity of 32 and 20.6 m/h, respectively, can be estimated. In correspondence with the other monitored springs (Pietrarossa, Sablici, Moschenizze, Sardos and Timavo), the tracer was not detected. This means that there is no connection between any of these monitored springs and swallow hole Sw-02.

Regarding the other smaller springs close to Pz_M and MC, they are placed in an area inhabited and are unreachable, so no information can be addressed regarding the tracer path.

The Mucille depression can be divided into 2 sectors characterised by different hydrodynamics. In sector A (the Selz settlement, Fig. 6A) a perennial spring S-02 and a channel draining water to swallow hole Sw-01 are present. Part of the waters are also swallowed by the S-01 estavelle. During floods, a bypass activates and spring waters are thus drained by swallow hole Sw-02. The three artificial lakes (Fig. 6 letter Q) in the north-western part of the study area can be considered storage basins. They accumulate waters only during floods and release them after the flood peak towards Sw-01 and Sw-02. Sector B (the riding school depression, Fig. 6B) is normally dry. Only under floods at an elevation of about 6.1 m a.s.l. temporary spring S-04 activates and its waters, collected in the most depressed parts of the area, flow towards swallow hole Sw-03. Figure 6 describes the areas affected by the December 2017 flood. At that time, the water level in area A reached an elevation of 7.5 m a.s.l., while in area B the level was about 6 m a.s.l. This difference is essentially related to the different flow rates characterising S-02 and S-04 and the drainage capacity of the swallow holes.

To quantify the flows involved in the system, and in particular to verify the functionality of swallow hole Sw-02, no longer considered active by the population, a total of 13 discharge measurements were carried out under different hydrogeological conditions (Table 1). It can be seen from the data analyses that the maximum discharge measured at the springs is 134.9 l/s, at the Sw-01 is 81.7 l/s and at the Sw-02 is 85.8 l/s. In the case of Sw-03, it was possible to perform a measurement only during the flood with a peak value of 30 l/s, which occurred on December 2017. During very low-flow period, only spring S-02 is active with flow rates of a few l/s.

When the water level is higher than 6.4 m a.s.l., an estimate of the swallow hole discharge can be computed using the proposed model. During the 3-year monitoring period we analysed 4 high water level periods: November 2017–January 2018, February 2019, May 2019 and November–December 2019 (Table 2 and Figs. 7 and 8). The analysis performed for each of the 4 identified situations is described in detail below.

EVENT 1: November 2017–January 2018 (Fig. 7 Event 1, Table 2)

After a particularly rainy September with a cumulative precipitation of over 230 mm, October saw only one significant precipitation of 44 mm on the 23rd October. In November there was a relatively low flow with levels of 4.8 m a.s.l. (S20). The period between November and mid-December

Table 1 Discharge measurements and estimates carried out under different hydrogeological conditions at the swallow holes Sw-01, Sw-02 and Sw-03 and in correspondence with the channels draining the quarry lakes and the springs

Water point	Data	Method	Discharge [l/s]	Water level S20 [m asl]
Sw-02	2/8/2019	Measured	85.8	6.40
Sw-02	2/13/2019	Measured	73.3	5.75
Sw-02	2/15/2019	Measured	63.1	5.48
Sw-02	2/18/2019	Measured	6.7	5.22
Sw-02	2/20/2019	Measured	n.d	5.11
Sw-02	2/26/2019	Measured	n.d	4.85
Sw-02	5/24/2019	Measured	65.1	5.66
Sw-02	6/4/2019	Measured	80.8	6.31
Sw-01	2/15/2019	Estimated	67.0	5.48
Sw-01	2/18/2019	Estimated	77.3	5.22
Sw-01	2/20/2019	Measured	70.6	5.11
Sw-01	2/26/2019	Measured	25.8	4.85
Sw-01	5/24/2019	Estimated	81.7	5.66
S-01 + S-02 + S-03	2/15/2019	Measured	130.1	5.48
S-01 + S-02 + S-03	2/18/2019	Measured	84.0	5.22
S-01 + S-02 + S-03	2/20/2019	Measured	70.6	5.11
S-02	2/26/2019	Measured	49.4	4.85
S-01 + S-02 + S-03	5/24/2019	Measured	134.9	5.66
Sw-03	12/19/2017	Measured	30.0	7.57
S-01	2/26/2019	Measured	-23.6	4.85

was characterised by considerable rainfall, which took to a progressive rising in the lake water level resulting in a series of successive floods of the Mucille polje. The main event occurred during mid-December with a cumulative rainfall of 153 mm. On December 11th, over a period of 14 h, the water level of the lake rose 1 m, which, on the basis of the computations made by using the proposed model corresponded to a maximum surplus (Q_{diff} Max–difference recorded between inflow and outflow) of +881 l/s. In the following days, new rainfall events took the lake water level to a value of 7.5 m a.s.l. which corresponded to a stored volume of 153,745 m^3. After the 18th December, when the outflow was bigger than the inflow, the lake water level started to lower with a maximum value of Q_{diff} Min as -233 l/s. In eight days the lake empties and the water returns to the canals (water level below 6.4 m a.s.l.).

EVENT 2: February 2019 (Fig. 7 Event 2, Table 2)

At the beginning of 2019 between the 1st and 3rd of February, an intense rainfall occurred with a cumulative rainfall of 87 mm. This event was preceded by a precipitation of 15 mm on January 28th. On February 2nd, over a period of 17 h, the water level of the lake rose 1 m which, on the basis of the computations made by using the proposed model corresponded to a maximum surplus (Q_{diff} Max) of approximately +300 l/s. In correspondence with the flood peak (6.4 m a.s.l.), the waters remained channelised

flowing towards the swallow holes and the stored volume was 38,794 m^3. Suddenly the water level started to lower with a maximum value of Q_{diff} Min as − 89 l/s. The area emptied with an almost progressive lowering over a period of 14 days ending on February 24th.

EVENT 3: May 2019 (Fig. 8 Event 3, Table 2)

No significant rainfall was recorded between February and April 2019, thus the level of Lake Mucille dropped to values of 4.6 m a.s.l. Subsequently, a series of minor rainfall events with values between 15 and 40 mm led to a slight rise in the lake level to values of about 5.5 m a.s.l. From 27th–30th May, the study area was affected by intense precipitation with a cumulative rainfall of 80 mm. On May 28th the level of the lake rose 50 cm over a period of 22 h, and on May 30th the maximum surplus (Q_{diff} Max) was + 331 l/s. In correspondence with the flood peak (6.6 m a.s.l.), the stored volume was 51,525 m^3. After May 31st, the lake water level started to lower with a maximum value of Q_{diff} Min as − 124 l/s. During this event, two discharge measurements were carried out at the springs and in the channel upstream from Sw-02 with a flow rate of 135 l/s and 65.1 l/s, respectively. The measures done allowed for an estimation of the flow rate value of Sw-01 which was 81.7 l/s.

Table 2 Summary of the flooding events

EVENT 1: November 2017–January 2018

Rainfall event		Water level		Max volume stored [m³]	Q_{diff} max		Q_{diff} min	
Date	[mm]	Peak date	Max [m a.s.l.]		Max date	Max [l/s]	Max date	Max [l/s]
06/11/2017–13/11/2017	65	11/14/2017	6.1	20,493	11/14/2017	222	11/15/2017	-88
26/11/2017–01/12/2017	76	12/4/2017	6.2	25,518	12/1/2017	148	12/6/2017	-81
09/12/2017–16/12/2017	153	12/18/2017	7.5	153,744	12/12/2017	881	12/25/2017	-233
27/12/2017–03/01/2018	97	1/3/2018	7.0	86,174	1/2/2018	379	1/9/2018	-121
01/02/2018–03/02/2018	60	2/6/2018	5.8	10,420	2/3/2018	67	2/8/2018	-4

EVENT 2: February 2019

Rainfall event		Water level		Max volume stored [m³]	Q_{diff} max		Q_{diff} min	
Date	[mm]	Peak date	Max [m a.s.l.]		Max date	Max [l/s]	Max date	Max [l/s]
01/02/2019–03/02/2019	87	2/7/2019	6.4	38,794	2/3/2019	299	2/9/2019	-89

EVENT 3: May 2019

Rainfall event		Water level		Max volume stored [m³]	Q_{diff} max		Q_{diff} min	
Date	[mm]	Peak date	Max [m a.s.l.]		Max date	Max [l/s]	Max date	Max [l/s]
19/05/2019–21/05/2019	38	5/22/2019	5.6	6,294	5/22/2019	39	5/27/2019	-18
27/05/2019–30/05/2019	80	5/31/2019	6.6	51,525	5/30/2019	331	6/4/2019	-124

EVENT 4: November–December 2019

Rainfall event		Water level		Max volume stored [m³]	Q_{diff} Max		Q_{diff} Min	
Date	[mm]	Peak date	Max [m a.s.l.]		Max date	Max [l/s]	Max date	Max [l/s]
02/11/2019–09/11/2019	128	11/9/2019	6.1	20,884	11/9/2019	164	11/11/2019	-40
11/11/2019–20/11/2019	189	11/21/2019	7.8	220,233	11/20/2019	753	11/24/2019	-273
19/12/2019–22/12/2019	79	12/25/2019	7.0	91,665	12/23/2019	567	12/31/2019	-179

Cumulative data regarding the rainfall events and their time spans; water level measured in correspondence with the S20 piezometer; maximum stored volume evaluated by means of the proposed model; Q_{diff} max as the positive difference between inflow and outflow and the relative date of occurrence; Q_{diff} min as the negative difference between inflow and outflow and the relative date of occurrence

EVENT 4: November–December 2019 (Fig. 8 Event 4, Table 2)

The particularly heavy rainfall in autumn 2019 came after a month characterised by slight rainfalls, never exceeding 6 mm with a cumulative value of 47 mm. From November 2nd to 9th there were three events with rainfall between 40 and 45 mm (128 mm cumulative) causing the lake level to rise from 4.6 to 6.1 m a.s.l. Subsequently, a further 189 mm of rainfall was observed over 10 days. On November 20th the maximum surplus (Q_{diff} Max) was +753 l/s. In correspondence with the flood peak (7.8 m a.s.l.), the stored volume of the lake was evaluated at 220,233 m³. After November 21st, the lake water level started to lower with a maximum value of Q_{diff} Min as − 273 l/s. Between 19th and 22nd December another intense precipitation occurred with a cumulative rainfall of 79 mm. The water level increased up to 7.0 m a.s.l. and occurred 14 days to restore the water level below 6.4 m a.s.l.

Discussion

In order to identify the most appropriate mitigation measures to reduce the flood risk for the buildings in the proximity of the Mucille depression, it is essential to have a clear idea of the polje hydrodynamics, and in particular to estimate the discharge values net of the outflows from the swallow holes. In recent years, various model approaches have been used to reproduce the flood dynamics of karst depressed areas by monitoring physico-chemical parameters (López-Chicano et al. 2002; Blatnik et al. 2019, 2020), water balance (Kovačič 2010; Naughton et al. 2015), hydraulic models (Gill et al. 2013a, b), and numerical models (Mayaud et al. 2019). With the aim of identifying the best mitigation measures for the Mucille area in case of floods, a model was developed for area A to properly estimate its recharge, the stored water volume and the related regression curve. As far as area B is concerned, from the observations made, even at the peak of the flood, swallow hole Sw-03 functions and
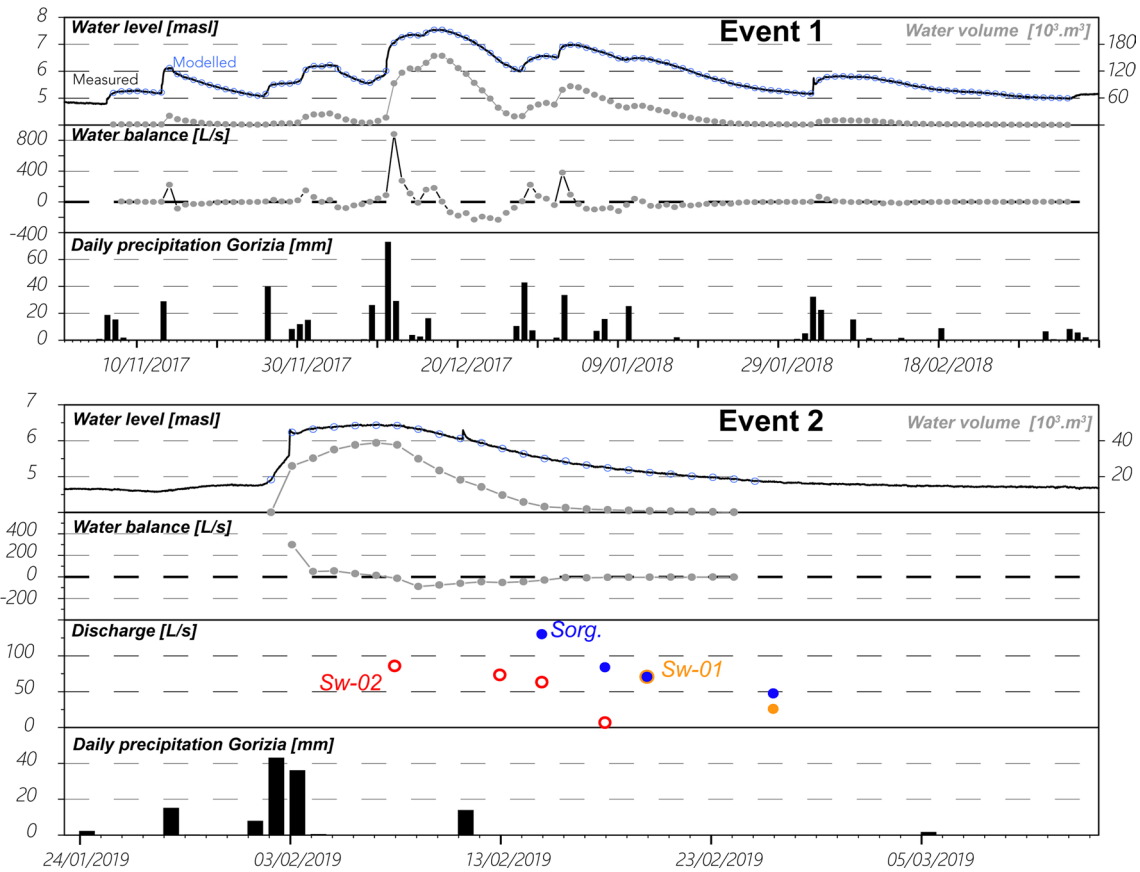
Fig. 7 Hydrological model for area A in the Mucille polje related to flood events no. 1 and 2. In the uppermost plot of both events, black line is related to the measured water level in the S20 (Measured), blue circles represent the daily water level used by the model (Modelled). During Event 2, several discharge measurements were realised in three different points: swallow hole Sw-02 is depicted in red, swallow hole Sw-01 is depicted in orange, and the springs are depicted in blue

manages to drain the waters coming from temporary spring S-04. Only when the static water level in sector A exceed 8 m a.s.l., an overflow affected sector B, the location of the riding school, first flooding the most depressed areas located at elevations slightly more than 7 m a.s.l.

From the results of the discharge measurements that can be realised when the waters are lower than 6.4 m a.s.l. it emerged that Sw-01 and Sw-02 function regularly, draining more than 80 l/s each. The test done on February 26th during low groundwater conditions made it possible to observe that S-01 behaves like an estavelle: when the water level is lower than 5 m a.s.l., it serves as a swallow hole; when the water level is higher than this value, it serves as a spring. The discharge drained by the swallow holes is not only linked to the discharge of the spring and to the water level of the lake, but also to the ability of the aquifer to drain the waters. As observed in the recordings in Sw-01, there is no direct link between the water level at Mucille and the swallow hole discharges. If we consider, for example, the recording from 15th February 2019, the discharge of the Sw-01 was 67.0 l/s with a water level of 5.48 m a.s.l.

Three days later the discharge was 77.3 l/s with a water level of 5.22 m a.s.l. This apparent inconsistency is evident only if we focus on the discharge value of each single swallow hole, instead we have to consider the discharge of the whole area. On 15th February the discharge value was 130.1 l/s while three days later it was of 84 l/s.

The proposed model permits to verify the functioning of the swallow hole even during floods, also when direct measurements are not possible due to the flooding of the area. The value of Q_{diff} Min (difference between Inflow and Outflow) represents the minimum outflow from the Mucille lake and consequently the discharge of the swallow holes. As estimated for November 2019 flood, the swallow holes have a discharge of more than 270 l/s, which is not enough to drain the spring discharge, which in turn can reach at least a value of at least 1 m³/s. As a consequence, in certain situations the lake water level could rise very fast (more than 7 cm/h), which occurred during the November 2017 flood. The fast rising of the lake waters obviously represents a serious hazard for those living in the Selz settlement.
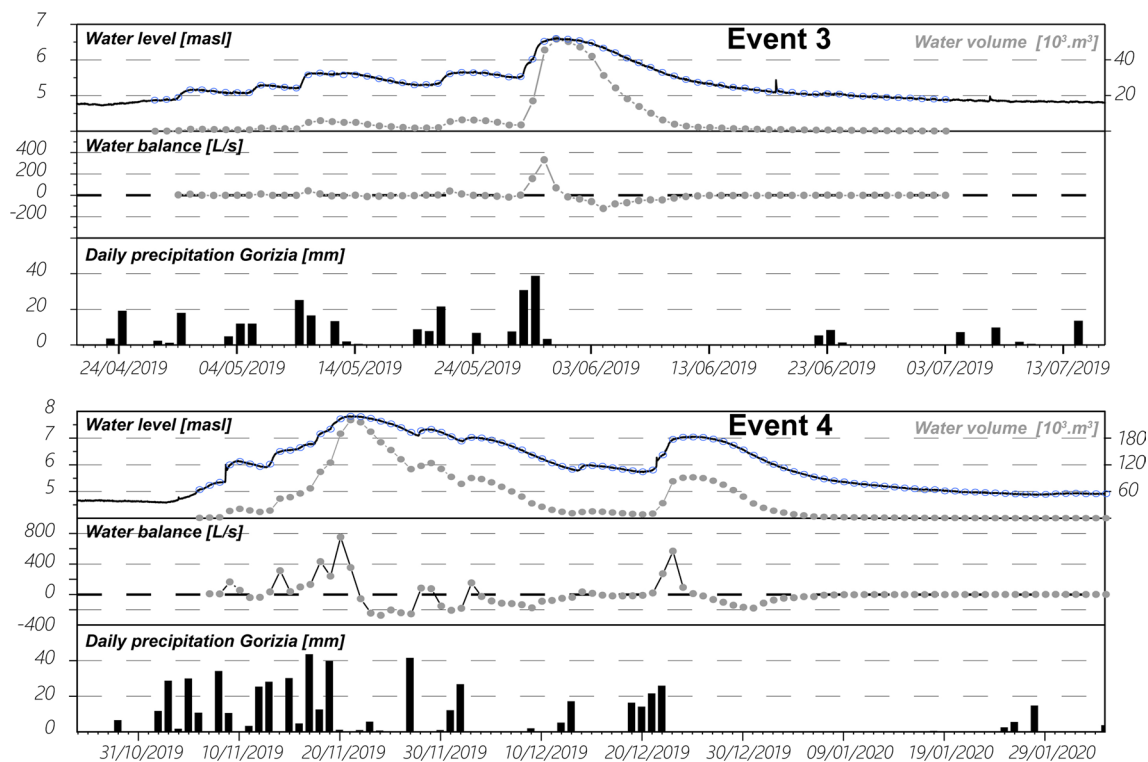
Fig. 8 Hydrological model for area A in the Mucille polje related to flood events no. 3 and 4. In the uppermost plot of both events, black line is related to the measured water level in the S20 (Measured), blue circles represent the daily water level used by the model (Modelled)

This situation is made even more serious by the fact that studies on climate change carried out for the Friuli Venezia Giulia Region (ARPA 2018) indicate an increase in the frequency of extreme events in the next hundred years. The most intense precipitation usually occurs in autumn. The two most important events recorded during the monitoring campaign (autumn 2017 and 2019) show that the flooding of the Mucille area occurs jointly not with a single isolated precipitation, but with a period of approximately one month with a series of precipitation of 20–40 mm. These precipitation events saturate the soil, also favouring flooding with a triggering event lasting 3–5 days, characterised by cumulative precipitation of more than 100 mm (approximately 130 mm in 2017 and 2019). In both analysed events, the 30-day cumulative precipitation was more than 300 mm. The levels reached 7.5 and 7.8 m a.s.l. and led the lake waters to lap the buildings located at the lowest altitudes. On the basis of this information, the rainfall data from the Gorizia monitoring station, which covers 100 years of measurements from 1919 to 2019, with an interruption at the end of the 1940s, were analysed, highlighting the frequency of events exceeding 350 mm of monthly precipitation, i.e. those that can generate high-risk situations for the houses.

From 1919 to 2019, 19 events were recorded with a 30-day cumulative precipitation of more than 350 mm. The distribution of the events is not uniform over the period. Nine events were observed from 1919 to 1990, whereas an average annual precipitation over the period was 1,370 mm/y. Ten events occurred in the last 30 years when average annual precipitation over the period was 1,330 mm/y. Eight of these occurred between 2000 to 2019, when average annual precipitation was 1,320 mm/y. This increase in the events is evidence of changes in the precipitation regime.

Conclusions

In karst settings where surface water is scarce, areas where freshwaters are abundant represent a resource and have therefore been increasingly anthropised over time, sometimes even modifying the natural landscapes and the environments. Often land restoration measures were aimed at regulating the waters and reducing wetlands, increasing construction, agriculture and land used for pasture forcing the water into defined spaces. With the increase in the magnitude and frequency of extreme rainfall events, ongoing climate change undermines these sensitive environments. This is also the case in the Friuli Venezia Giulia Region and the Classical Karst Region, for which all forecast models indicate a 20–30% increase in rainfall during winter, a significant increase in temperature and also resulting higher evapotranspiration and a change in the rainfall regime with

an increase in extreme events. From this perspective, the Mucille area is exemplary, with an intensification of extreme events (30-day cumulative precipitation of more than 350 mm) within the considered time-period of 1919–2020. Since 2000, the flooding problem has become increasingly critical, hence the need for the municipality to have insight into the area in order to better plan mitigation measures for safety and risk reduction. The hydrodynamics of the Mucille polje were analysed from 2017 to 2020 by using different approaches. A monitoring network was set up which provided an understanding of the water flow patterns. Several discharge field surveys defined the water quantities involved and verified the efficiency of the swallow holes. The hydrogeological model made it possible to quantify the flow rates even during floods. In particular, swallow hole Sw-02, which according to popular opinion had stopped working due to the expansion of the agricultural area, and the presence of a drainage system for the aqueduct pipes, was the subject of more in-depth investigations including geophysical surveys. Direct and indirect investigations confirmed its functionality, although it is not possible to establish whether or not there has been a reduction in flow rate, which to date can be estimated at least 250 l/s for both swallow holes (Sw-01 and Sw-02). Based on these latter considerations, the increase in extreme phenomena observed by the inhabitants cannot be blamed on the works which partially reduced the pertinence area of swallow hole Sw-02, but on ongoing climate change.

All the preliminary studies are focused on the possibility to increase its current drainage. There are several options:

(1) a drainage channel (about 1.5 km in length), oriented towards Pietrarossa Lake, which activates when water levels exceed 6 m a.s.l. This solution partially maintains the naturality of the area and, at the same time, preserves the safety for infrastructures and inhabited areas; according to our studies, the channel should have a flow rate of at least $1 m^3/s$;

(2) embankments positioned downstream from the built-up area and upstream from the lake. This is an impacting construction which should reach an elevation of 9 m a.s.l. to be functional;

(3) Sw-02 restoration up to its naturality and full functionality could decrease the flooding rate in the area, increasing the drainage of the waters.

(4) frequent maintenance activities aimed at cleaning vegetation from the swallow hole area, which tends to accumulate causing obstructions.

The proposed Solutions 1 and 2 are decisive, but points 3 and 4 could most certainly assist in improving the drainage capacity, increasing the emptying process. One must note that a potential drawback to solutions 3 or 4 have a weak point in the drainage capacity which in turn is strongly linked to the level of the groundwater. These solutions, although not guaranteeing a complete answer to the problem, are certainly the most cost-effective with a low environmental impact and would have an immediate effect.

Declarations

Conflict of interest The authors declare no competing interests.

References

ARPAFVG (2018) Studio conoscitivo dei cambiamenti climatici e di alcuni loro impatti in Friuli Venezia Giulia. PRIMO REPORT – marzo 2018 Supporto alla predisposizione di una strategia regionale di adattamento ai cambiamenti climatici e per le azioni di mitigazione. ARPAFVG, p 342

Blatnik M, Mayaud C, Gabrovšek F (2019) Groundwater dynamics between Planinsko polje and springs of the Ljubljanica river, slovenia. Acta Carsologica 48(2):199–226. https://doi.org/10.3986/ac.v48i2.7263

Blatnik M, Mayaud C, Gabrovšek F (2020) Supplement to the paper "Groundwater dynamics between Planinsko polje and springs of the Ljubljanica river, Slovenia" from Blatnik et al. (2019). Acta Carsologica 49(1):143–147. https://doi.org/10.3986/ac.v49i1.8721

Calligaris C, Mezga K, Slejko FF, Urbanc J, Zini L (2018) Groundwater characterization by means of conservative (d18O and d2H) and non-conservative (87Sr/86Sr) isotopic values: the Classical Karst Region aquifer case (Italy–Slovenia). Geosciences 8:321. https://doi.org/10.3390/geosciences8090321

Calligaris C, Galli M, Gemiti F, Piselli S, Tentor M, Zini L, Cucchi F (2019a) Electrical Conductivity as a tool to evaluate the various recharges of a Karst aquifer. ROL 47:13–17

Calligaris C, Casagrande G, Iervolino D, Lippi F, Olivo P, Ramani M, Treu F, Zini L (2019b) Water–budget as a tool to evaluate the sustainable use of groundwater resources (Isonzo Plain, NE Italy). ROL 47:7–12. https://doi.org/10.3301/ROL.2019.02

Cancian G (1987) L'idrologia del Carso goriziano-triestino tra l'Isonzo e le risorgive del Timavo. Studi Trentini Di Scienze Naturali 64:77–98

Civita M, Cucchi F, Eusebio A, Garavoglia S, Maranzana F, Vigna B (1995) The river Timavo: an important supplementary water resource which needs to be protected and regained. Acta Carsologica 24:169–186

Cucchi F, Piano C (2013) Carta geologica del Carso Classico (tratta dalla Carta di sintesi geologica alla scala 1:10.000 – Progetto GEO-CGT) e Brevi Note Illustrative della Carta Geologica del Carso Classico Italiano, con F. Fanucci, N. Pugliese, G. Tunis, L. Zini. Direzione centrale ambiente energia e politiche per la montagna. Servizio Geologico, Regione Autonoma Friuli Venezia Giulia, Trieste, Italy

Cucchi F, Zini L, Calligaris C (2015) Le acque del Carso Classico, Progetto HYDROKARST. EUT, ISBN 978-88-8303-621-7

Doctor D (2008) Hydrologic connections and dynamics of water movement in the classical karst (kras) aquifer: evidence from frequent chemical and stable isotope sampling. Acta Carsologica 3(1):101–123

Doctor DH, Lojen S, Horvat M (2000) A stable isotope investigation of the Classical Karst aquifer: evaluating karst groundwater components for water quality preservation. Acta Carsologica 29(1):79–82

EEA (European Environment Agency) (2016) Flood phenomena. http://www.eea.europa.eu/data-and-maps/data/european-past-floods

Filippini M, Squarzoni G, De Waele J, Fiorucci A, Vigna B, Grillo B, Riva A, Rossetti S, Zini L, Casagrande G, Stumpp C, Gargini A (2018) Differentiated spring behavior under changing hydrological conditions in an alpine karst aquifer. J of Hydrol 556:572–584. https://doi.org/10.1016/j.jhydrol.2017.11.040

Ford DC, Williams PW (2007) Karst hydrogeology and geomorphology. John Wiley & Sons, Chichester, p 562

Gabrovšek F, Peric B (2006) Monitoring the flood pulses in the epiphreatic zone of karst aquifer: the case of Reka river system, Karst plateau. SW Slov Acta Carsologica 35(1):35–45

Gabrovšek F, Peric B, Kaufmann G (2018) Hydraulics of epiphreatic flow of a karst aquifer. J of Hydrol 560:56–74. https://doi.org/10.1016/j.jhydrol.2018.03.019

Gemiti F (1994) Indagini idrochimiche alle risorgive del Timavo. Atti e Memorie Della Commissione Grotte "e. Boegan" 30:73–83

Gemiti F, Licciardello M (1977) Indagini sui rapporti di alimentazione delle acque del Carso triestino e goriziano mediante l'utilizzo di alcuni traccianti naturali. Annali Gruppo Grotte Ass 30:643–661

Gill LW, Naughton O, Johnston PM (2013a) Modelling a network of turloughs in lowland karst. Water Resour Res 49(6):3487–3503

Gill LW, Naughton O, Johnston PM, Basu B, Ghosh B (2013b) Characterisation of hydrogeological connections in a lowland karst network using time series analysis of water levels in ephemeral groundwater-fed lakes (turloughs). J Hydrol (amst) 499:289–302

Gracia FJ, Gutiérrez F, Gutiérrez M (2003) The Jiloca karst polje-tectonic graben (Iberian Range. NE Spain). Geomorphology 52(3–4):215–231

Hirabayashi Y, Mahendran R, Koirala S, Konoshima L, Yamazaki D, Watanabe S, Hyungjun K, Shinjiro K (2013) Global flood risk under climate change. Nat Clim Change Lett 3:816–821. https://doi.org/10.1038/NCLIMATE1911

Jurkovšek B, Biolchi S, Furlani S, Kolar-Jurkovšek T, Zini L, Jež J, Tunis G, Bavec M, Cucchi F (2016) Geology of the classical karst region (SW Slovenia–NE Italy). J Maps 12(1):352–362. https://doi.org/10.1080/17445647.2016.1215941

Kovačič G (2010) An attempt towards an assessment of the Cerknica polje water balance/ Poskus ocene vodne bilance Cerkniškega polja. Acta Carsologica 39(1):39–50

Kvočka D, Falconer RA, Bray M (2016) Flood hazard assessment for extreme flood events. Nat Hazards 84:1569–1599. https://doi.org/10.1007/s11069-016-2501-z

Long D, Shen Y, Sun A, Hong Y, Longuevergne L, Yang Y, Li B, Chen L (2014) Drought and flood monitoring for a large karst plateau in Southwest China using extended GRACE data. Remote Sens Environ 155:145–160

Lopez N, Spizzico V, Parise M (2009) Geomorphological, pedological, and hydrological characteristics of karst lakes at Conversano (Apulia, southern Italy) as a basis for environmental protection. Environ Geol 58(2):327–337

Lopez-Chicano M, Calvache ML, Martın-Rosales W, Gisbert J (2002) Conditioning factors in flooding of karstic poljes—the case of the Zafarraya polje (South Spain). CATENA 49:331–352

Margiotta S, Parise M (2019) Hydraulic and geomorphological hazards at wetland geosites along the eastern coast of Salento (SE Italy). Geoheritage 11(4):1655–1666

Mayaud C, Gabrovšek F, Blatnik M, Petrič M, Ravbar N (2019) Understanding flooding in poljes: a modelling perspective. J Hydrol 575:874–889

Mihevc A, Mihevc R (2021) Morphological characteristics and distribution of dolines in Slovenia, a study of a Lidar-based doline map of Slovenia. Acta Carsologica 50(1):11–36. https://doi.org/10.3986/ac.v50i1.9462

Morrissey PJ, McCormack T, Naughton O, Johnston PM, Gill LW (2020) Modelling groundwater flooding in a lowland karst catchment. J Hydrol 580:124361. https://doi.org/10.1016/j.jhydrol.2019.124361

Mosetti F, D'Ambrosi C (1963) Alcune ricerche preliminari in merito a supposti legami di alimentazione fra il Timavo e l'Isonzo. Boll Geofis Teor Appl 5:69–83

Naughton O, Johnston PM, McCormack T, Gill LW (2015) Groundwater flood risk mapping and management: examples from a lowland karst catchment in Ireland. J Flood Risk Manag 10:53–64. https://doi.org/10.1111/jfr3.12145

Parise M (2015) Karst geo-hazards: causal factors and management issues. Acta Carsologica 44(3):401–414

Parise M, Closson D, Gutiérrez F, Stevanović Z (2015) Anticipating and managing engineering problems in the complex karst environment. Environ Earth Sci 74(12):7823–7835. https://doi.org/10.1007/s12665-015-4647-5

Ravbar N, Mayaud C, Blatnik M, Petrič M (2021) Determination of inundation areas within karst poljes and intermittent lakes for the purposes of ephemeral flood mapping. Hydrogeol J 29(1):213–228. https://doi.org/10.1007/s10040-020-02268-x

Samez D, Casagrande G, Cucchi F, Zini L (2005) Idrodinamica dei laghi di Doberdò e di Pietrarossa (Carso Classico, Italia). Relazioni con le piene dei fiumi Isonzo, Vipacco e Timavo. Atti e Mem Commissione Grotte "e. Boegan" 40:133–152

Tabari H (2020) Climate change impact on flood and extreme precipitation increases with water availability. Sci Rep 10:13768. https://doi.org/10.1038/s41598-020-70816-2

Timeus G (1928) Nei misteri del mondo sotterraneo: risultati delle ricerche idrogeologiche sul Timavo 1895–1914, 1918–1927. Atti e Mem Commissione Grotte "e. Boegan" 22:117–133

Treu F, Zini L, Zavagno E, Biolchi S, Boccali C, Gregorič A, Napolitano R, Urbanc J, Zuecco G, Cucchi F (2017) Intrinsic vulnerability of the Isonzo/Soča High plain aquifer (NE Italy–W Slovenia). J Maps 13(2):799–810

Van Essen Instruments (2023) Technology sheet. https://www.vanessen.com/product-category/data-loggers/. Accessed 20 Jan 2023

Velić I (2007) Stratigraphy and palaeobiogeography of Mesozoic Benthic foraminifera of the Karst Dinarides (SE Europe). Geol Croat 60(1):1–113

Vižintin G, Ravbar N, Janež J, Koren E, Janež N, Zini L, Treu F, Petrič M (2018) Integration of models of various types of aquifers for water quality management in the transboundary area of the Soca/Isonzo River basin (Slovenia/Italy). Sci Total Environ 619–620:1214–1225

Vlahović I, Tišljar J, Velić I, Matičec D (2005) Evolution of the Adriatic carbonate platform: palaeogeography, main events and depositional dynamics. Palaeogeogr Palaeoclimatol Palaeoecol 220:333–360

Watlet A, Van Camp M, Francis O, Poulain A, Rochez G, Hallet V, Quinif Y, Kaufmann O (2020) Gravity monitoring of underground flash flood events to study their impact on groundwater recharge and the distribution of karst voids. Water Res Res 56(4):26673. https://doi.org/10.1029/2019WR026673

Zini L, Calligaris C, Zavagno E (2014) Classical Karst hydrodynamics: a sheared aquifer within Italy and Slovenia. Evolving water resources systems: understanding predicting and managing water-society interactions, 364th edn. IAHS Publication, pp 499–504. https://doi.org/10.5194/piahs-364-499-2014

Zini L, Calligaris C, Cucchi F (2015) The challenge of tunneling through Mediterranean karst aquifers: the case study of Trieste (Italy). Environ Earth Sci 74:281–295. https://doi.org/10.1007/s12665-015-4165-5

Zini L, Calligaris C, Cucchi F (2022) Along the hidden Timavo. Geol Field Trips Maps. https://doi.org/10.3301/GFT.2022.03